Industrial Crops & Products 168 (2021) 113565

Contents lists available at ScienceDirect

Industrial Crops & Products

journal homepage: www.elsevier.com/locate/indcrop

Two-step optimization of solid-state fermentation conditions of heilong48 soybean variety for maximum chlorogenic acid extraction yield with improved antioxidant activity

Nelson Dzidzorgbe Kwaku Akpabli-Tsigbe [a,b], Yongkun Ma [a,*], John-Nelson Ekumah [a,b], Juliet Osabutey [c,d], Jie Hu [a], Manqing Xu [a], Nana Adwoa Nkuma Johnson [a], Janet Quaisie [a]

[a] School of Food and Biological Engineering, Oversea College of Education, Jiangsu University, 301#, Xuefu Road, Zhenjiang, 212013, Jiangsu, PR China
[b] Department of Nutrition and Food Science, College of Basic and Applied Sciences, University of Ghana, P. O. Box LG 134, Legon, Ghana
[c] Department of Early Childhood Education, University of Education, P. O. Box 25, Winneba, Ghana
[d] Virtuous Experimental School, P. O. Box AH 106, Achimota-Accra, West Africa, Ghana

ARTICLE INFO

Keywords:
Chlorogenic acid
Solid-state fermentation
Soybean
Plackett-Burman design
Box-Behnken design

ABSTRACT

This study sought to establish an optimized solid-state fermentation (SSF) conditions for extraction of chlorogenic acid (CA) from heilong48 soybean (HS) variety using two-step process: Plackett–Burman Design (PBD) and Box-Behnken Design (BBD) systematically. Both designs revealed the significant screened and optimum SSF conditions as pH (5.02), incubation time (11.52 h), inoculation size (5.00 %) and liquid-solid ratio (0.67). CA yield (8.80 ± 0.08 mg/g), fermentation efficiency (31.29 ± 0.28 %), and antioxidant activity (DPPH) (77.45 ± 0.60 μmol AA eq/g dry sample) obtained were acceptable (desirability, 1.00). Both the relative errors and the residual standard errors obtained for the predicted and experimental values were less than 5%. Higher ($p < 0.05$) CA yield and DPPH were obtained for the *Lactobacillus casei* fermented HS variety (LCFHS) than that of the unfermented HS variety (RHSF). The effectiveness of the optimized SSF conditions on the degradation of the cell wall of HS variety was affirmed by Scanning electron microscopy (SEM), Atomic force microscopy (AFM) and Fourier transform infrared (FTIR) results. The optimized extraction process was feasible, and HS variety could be used for CA extraction.

1. Introduction

The consumption of legumes has received significant attention globally, due to their positive effect on chronic diseases (Magro et al., 2019). One of such legumes is soybean (*Glycine max* L.), a most valuable crop worldwide with notable health benefits. From their clinical studies, Rehal et al. (2019) assented to the several health benefits derived from the consumption of soybean. Soybean thus, play a promising role in the prevention and treatment of cancer, atherosclerosis, osteoporosis, and coronary heart disease (Miladinovic et al., 2012). Zhang et al. (2014) reported that the potential of soybean to decrease the risk of cardiovascular diseases and cancers is associated to some functional compound it contains. According to Correa Deza et al. (2019) and Miladinovic et al. (2012), the high isoflavone genistein (a phytoestrogen) content of soybean is responsible for its effectiveness in cancer prevention and suppression. Soybean is rich in saponin, protease inhibitors, phytic acid, and fiber (Miladinovic et al., 2012). It also contains chlorogenic acid (CA) [least mentioned (Pratt and Birac, 1979)] which has numerous health benefits. Nevertheless, in the scientific community, isoflavones are the most mentioned bioactive compound in soybean with a very great interest attached (Chen et al., 2012).

That notwithstanding, recent studies (Wang et al., 2018), reference to flavonoids, suggest that CA is a more powerful antioxidant. Wang et al. (2018) further indicated that CA is extensively applied in cardiovascular and age-related diseases prevention, as well as protection against ischemia-reperfusion. Some researchers (Ji et al., 2013) also reported that CA prevents the production of cancerous cells in the colon and liver of mice. In addition, Cho et al. (2010) found that CA ameliorates lipid metabolism in mice. Yun et al. (2012) stated that CA exhibits anti-bacterial, anti-inflammatory, and anti-diabetic activities. As a result, application of natural CA in medicine, pharmaceutics, chemicals, foods (preservation, nutraceuticals, functional foods, food additives),

* Corresponding author.
E-mail addresses: ndkakpablitsigbe@outlook.com (N.D.K. Akpabli-Tsigbe), mayongkun@ujs.edu.cn (Y. Ma).

https://doi.org/10.1016/j.indcrop.2021.113565
Received 14 January 2021; Received in revised form 20 April 2021; Accepted 22 April 2021
Available online 3 May 2021

and cosmetics at present is on the demand. However, CA is mostly extracted from coffee; an expensive cash crop which is not available/accessible all-year round, limiting its commercial production, and hence making it expensive to produce. Lately, for cost-effective production, other dietary plants sources such as sweet potato peel are being studied for CA extraction (Alves Filho et al., 2020).

Nonetheless, soybean (an economical crop, available/accessible all-year round, easy to store with long shelf-life) has not been investigated for CA extraction yet. Soybean is used in solid-state fermentation (SSF) to obtain value added food, produce enzyme, and antioxidant compounds (Correa Deza et al., 2019). However, application of SSF technology using *Lactobacillus casei* (Generally Recognized as Safe) for extraction of CA from soybean has not been studied. Lactic acid bacteria (LAB) contain the enzyme β-glucosidase which hydrolyses isoflavone glucosides to form isoflavone-aglycones (Correa Deza et al., 2019). Hence, LAB play a significant role in changing isoflavone profile and increasing its content during fermentation of soymilk. Sub-merged fermentation (SmF) is commonly used to study the behaviour of LAB; however, low concentrations of active compounds are normally obtained. Higher yields with better product characteristics are obtained with SSF than SmF (Martins et al., 2011). As a result, SSF, a process of growing microorganisms on solid materials without free liquid, has received more interest from researchers and has become an important alternative for yield improvement. Therefore, the aim of this study was to screen and optimize the significant SSF conditions for cost-effective extraction of maximum CA yield with high antioxidant activity from heilong48 soybean (HS) variety using *L. casei* starter culture.

2. Materials and methods

HS variety was purchased from Tianxia Agricultural and Sideline Products and Distribution Department, China. *L. casei* LC-122 was bought from Synbio Tech Inc. (Taiwan) and stored at 4 °C until use. Reagents and chemicals including potassium bromide (KBr), saline phosphate buffer (PBS), 2,2-diphenyl-1-picrylhydrazyl (DPPH), Folin-Ciocalteu reagent, sodium carbonate (Na_2CO_3), pure CA standard, gallic acid standard and de Man, Rogosa and Sharpe (MRS) agar used were bought from Sinopharm Chemical Reagent Co., Limited (China).

2.1. HS flour preparation

HS variety was pulverized with a hammer crusher (FC160; 380v 50hz, Shanghai traditional Chinese medicine machinery factory, China) and further sieved (65-inch, 0.25 mm bore diameter, Shaoxing Shangyu Huafeng hardware instruments Co., Ltd, China) into fine flour of particle size 0.25 mm. The final flour was bagged in zip-lock rubber in weights of 150 g and stored (−20 °C) for further studies.

2.2. Inoculum preparation

Lactobacillus casei LC122 was activated in MRS broth at 37 °C for 24 h (Li et al., 2020). The culture was centrifuged (Ruijiang RJ-TDL-50A, China) at 4000×*g* for 10 min (Feng et al., 2018). The supernatant was discarded and the bacterium cells rinsed in 0.10 % sterile saline (NaCl) solution. The inoculum concentration was estimated with a hemocytometer (version XB-K-250, Jianling Medical Device Co., China) and adjusted to 10^9 CFU/mL with 0.10 % sterile saline solution (Kwaw et al., 2017). The obtained suspension was used as starter culture or inoculum for SSF.

2.3. SSF of HS variety

Distilled water was added to 10 g HS flour (on dry matter basis) to obtain moisture contents of 20, 30 and 40 % in a 250 mL conical flask. The contents were mixed thoroughly and autoclaved for 15 min at 121 °C (Li et al., 2020). The mixture (after cooling to 25 °C) was inoculated with *L. casei* (1, 3 and 5%) containing cell population of 10^9 CFU/g, mixed thoroughly and then cultured at 30, 40 and 50 °C in a microbial incubator (SPX-250, Jintanshizhongdayiqichang, China) for 0, 24 and 48 h under static aerobic conditions. All fermented samples were stored (−20 °C) for further analysis.

2.4. Screening of SSF conditions using Plackett-Burman design (PBD)

PBD is used to screen significant variables from a multivariable system and to provide a basis for further optimization (Guo et al., 2018). In this study, PBD was used to screen the significant SSF factors out of five factors namely temperature, pH, incubation time, inoculation size and liquid to solid ratio, marked by the symbols; A, B, C, D and E respectively which might affect SSF process for maximum CA yield extraction. The study design comprised of a two [low (−1) level and high (+1) level] factorial design set to find the important parameters for the CA extraction through screening "n" different parameters in "n+1" [includes midpoint (0) level] experiments, giving 13 runs of independent experimental combinations. The main effect was computed as a difference between the average measurements of each parameter at the high (+1) and low (−1) levels. PBD was established on a first-order polynomial model:

$$Y = \beta_0 + \sum_{i=1}^{5} \beta_i X_i \quad (1)$$

where Y = response, β_0 = model intercept and β_i = variable estimates (Karlapudi et al., 2018; Plackett and Burman, 1946).

2.5. Optimization of selected screened SSF conditions with Box-Behnken design (BBD)

The optimization of SSF conditions for CA extraction was achieved with Response Surface Methodology (RSM). Using BBD, the effect of the respective factors or parameters on the CA extraction was evaluated having CA yield, fermentation efficiency and DPPH as the dependent variables. The four important SSF conditions [pH (X_1), IT (X_2), IS (X_3) and L–S ratio (X_4)] selected by PBD were optimized using BBD for maximum CA yield extraction from HS variety. A BBD of four-factor-three-level (comprising of 29 experimental runs: 24 factorial and 5 mid runs) was applied based on preliminary experiments of A (30–50 °C), B (5–7), C (0–96 h), D (1–5%) and E (0.25–1.50). A second-order polynomial model was fitted to correlate the relationship of each factor to the response. The equation was:

$$Y = \beta_0 + \sum_{(i=1)}^{3} \beta_1 X_i + \sum_{i=1}^{2} \sum_{(j=i+1)}^{3} \beta_{ij} X_i X_j + \sum_{(i=1)}^{3} \beta_{ii} X_i^2 \quad (2)$$

Where Y = predicted response variable, β_0 = intercepts, β_i = linear regression coefficients, β_{ii} = second-order regression coefficients and β_{ij} = interaction regression coefficients, all estimated by the model and X_i and X_j = values of the independent variables. The overall Desirability Index (DI) was the basis for selection of the optimized parameters according to the relation:

$$DI = \left[\prod_{i=1}^{3} d_i(y_i)\right]^{1/3} \quad (3)$$

Where d_i = DI (0 to 1) for the dependent variable and y_i = response.

2.6. Preparation of standard CA solution

The method of Adane et al. (2019) was used for the preparation of the standard solution and validated against Beer-Lambert's law.

2.7. DPPH assay

The antioxidant activity of the raw HS flour (RHSF) and *L. casei* fermented HS (LCFHS) extracts against DPPH was performed using the method described by Haida and Hakiman (2019). Briefly, aliquots of 1 mL RHSF and LCFHS extracts were added to 2 mL of 1 mM methanolic dilution of DPPH (1×10^{-3} M). The mixture after vortexing, was incubated in the dark for 30 min at 37 °C and absorbance taken at 517 nm against a blank in a UV-1600 spectrophotometer (Beijing Rayleigh analytical instrument, Beijing, China). The results were expressed in μmol ascorbic acid equivalents per gram (μmol AA eq/g) dry sample using ascorbic acid standard curve generated under same conditions. The linear range for ascorbic acid standard was 12.50–800.00 μg/mL ($r^2 = 1.00$).

2.8. Total phenolic acids (TPA) determination

TPA was determined by adhering to the method reported by Haida and Hakiman (2019). Briefly, 1 mL of LCFHS was added to 9 mL of distilled water in a test tube. Then, 1 mL of Folin–Ciocalteu phenol reagent was added to it and the mixture, by using a vortex, was mixed thoroughly. After 5 min, 10 mL of 7% sodium carbonate was added. Next, 4 mL of distilled water was added and the mixture was adjusted to 25 mL of final volume. The reaction mixture was incubated for 90 min at room temperature, and the absorbance was measured at 750 nm in a UV-1600 spectrophotometer (Beijing Rayleigh analytical instrument, Beijing, China). The TPA were expressed as mg of gallic acid equivalents per gram of LCFHS. A standard curve for gallic acid (as standard) in methanol was prepared using different concentrations (100–700 μg/ml).

2.9. CA determination

CA determination was done based on an advanced procedures (Adane et al., 2019). CA concentration was calculated against the standard solution using Beer Lambert's Law at the maximum wavelength (λ_{max} = 325 nm). CA and %CA contents of RHSF and LCFHS samples were calculated with Eq. (4) (Wondimkun et al., 2016) and Eq. (5) respectively:

$$\text{CA content (mg)} = \frac{[\text{conc (mg/L)}] \times [\text{total sample volume (mL)}]^2}{[\text{measured sample volume (mL)}] \times 1000} \quad (4)$$

$$\%\text{CA (w/w\%)} = \frac{[\text{calculated mass of CA (mg)}]}{[\text{mass of sample measured (mg)}]} \times 100\% \quad (5)$$

2.10. Direct extraction of CA in raw (unfermented) HS variety

40 mg of sieved HS flour was weighed and dissolved in 30 mL

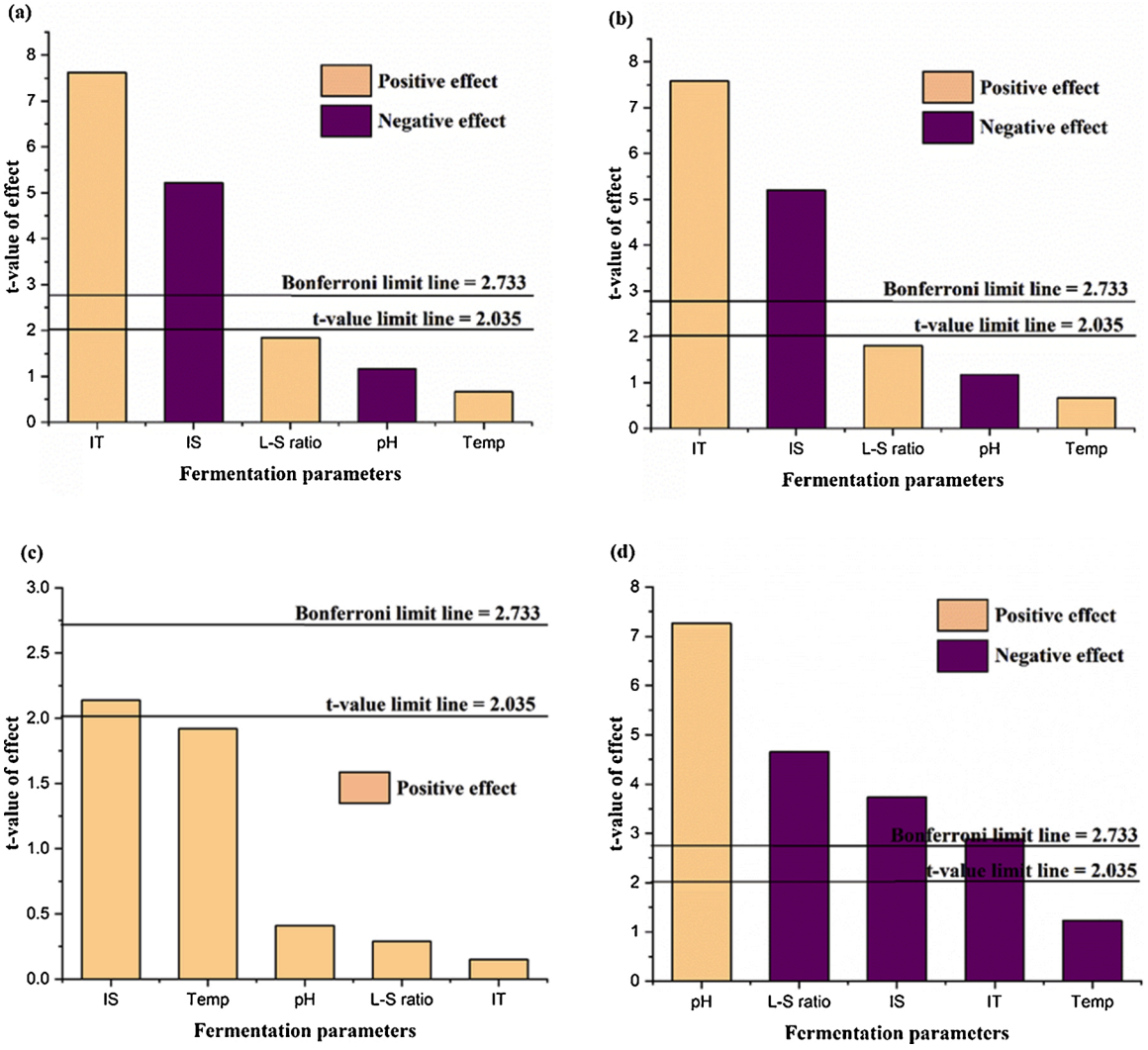

Fig. 1. Pareto chart for CA yields (a), fermentation efficiency (b), TPA (c), and DPPH (d) of LCFHS. Parameters with *t*-values greater than 2.035 (the critical value) were regarded significant statistically.

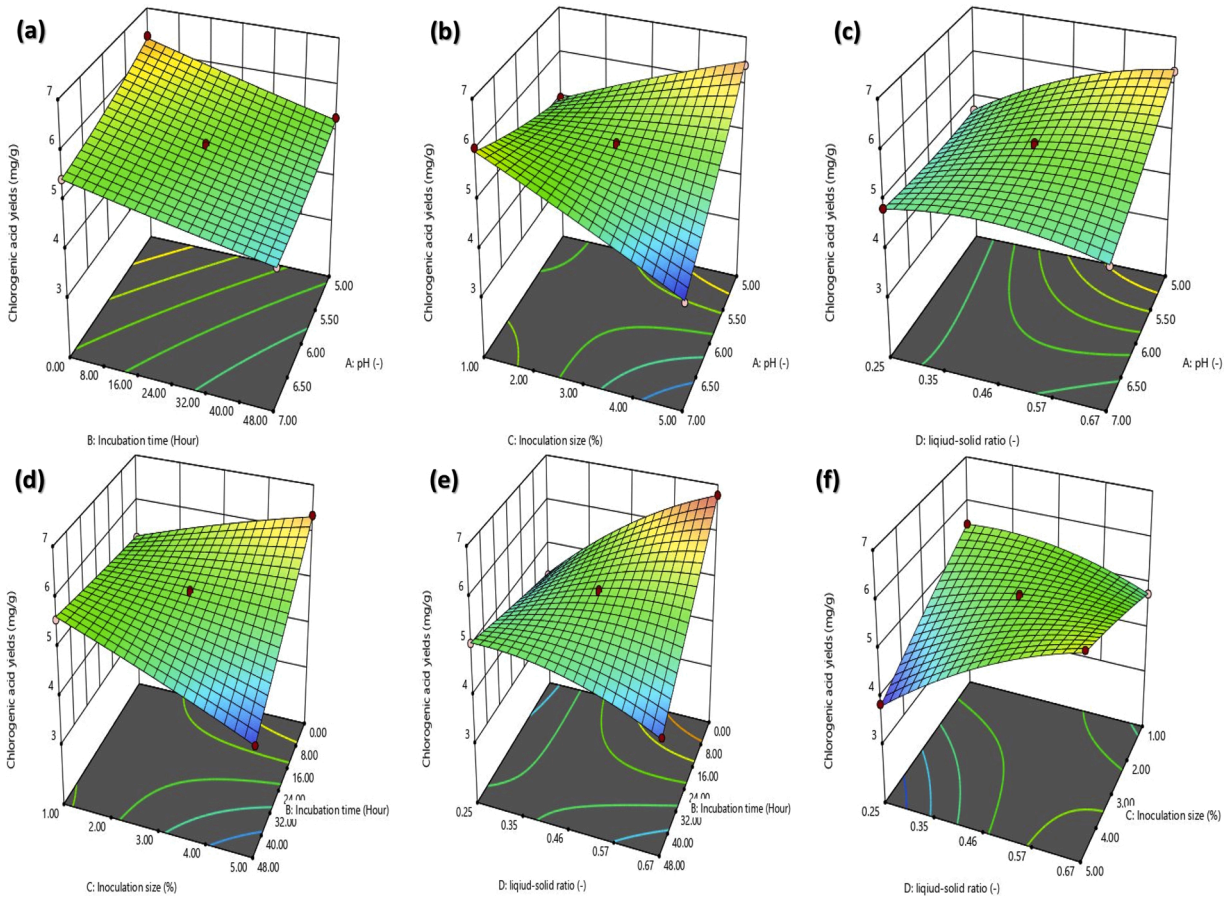

Fig. 2. Response surface and contour plots of interactive effects of pH, incubation time, inoculation size and liquid-solid ratio on the CA yield of HS variety.

distilled water in a 100 mL beaker. The solution was stirred for half an hour using magnetic stirrer (model C-MAG HS 7 S025, IKA, Germany) and heated (at 40 °C) to increase the solubility of CA in solution. The solution was filtered through double-loop qualitative filter paper (NO.1568, Ge Biotechnology Co., Ltd, China) to get rid of particles from solution. The filtrate containing CA was collected and measured to obtain volume of the sample extract. The absorbance of the measured sample extract was taken at 325 nm using UV-1601 spectrophotometer (Beijing Rayleigh Analytical Instrument Co. Ltd, China). CA and %CA were computed with Eqs. (4) and (5).

2.11. Fourier transform infrared (FTIR) analysis

FTIR spectroscopy was applied to determine the structure of LCFHS and RHSF samples according to the method of Musa et al. (2019).

2.12. Scanning electron microscopy (SEM) and Atomic force microscopy (AFM) analysis

The SEM method described by Musa et al. (2019) was used to study the structure of LCFHS and RHSF samples. The topography of LCFHS and RHSF samples were determined with the method outlined by Dabbour et al. (2020).

2.13. Statistical analysis

The experimental designs, as well as the statistical analysis for the optimization was achieved using Design Expert Software (version 11.0.5.0, STAT-EASE, Inc., Minneapolis, USA). The variables were screened using MINITAB v18.1 software (Minitab Inc., Pennsylvania, USA). The model accuracy was assessed using: The P-test, the coefficient of variation (CV), the lack of fit test, and the coefficient of determination (R^2) represented at $p < 0.05$, 0.01 and 0.001. All experimental analyses were performed in triplicates and data processed with MS Excel 2016 (Microsoft Corporation, Redmond, WA, USA). All graphs were constructed using OriginPro version 2018 (OriginLab Corporation, Northampton, MA, USA). The values were expressed as mean ± standard deviation and Tukeys' test was used for comparison of the means at $p < 0.05$.

3. Results and discussion

3.1. Effect of SSF conditions on CA extraction

IT had a positive *t*-value effect on CA yield and fermentation efficiency, indicating that increasing IT increased CA yield and fermentation efficiency. A negative *t*-value effect was obtained for IS on CA yield and fermentation efficiency suggesting that increasing IS decreased CA yield and fermentation efficiency. This implied that as the IS increased, the *t*-value of effect showed a significant opposing effect on CA yield and fermentation efficiency. Suggestive that a longer IT increased CA yield as it gave *L. casei*, optimum period for adaptation to the conditions of the fermenting medium, resulting in proliferation, and in turn degradation of the cell walls of the HS to release considerable quantity of CA during fermentation (Su et al., 2018). Mostly, hydroxycinnamic acids exist in linked-form with cell walls, however, the soluble compounds are mainly located inside the plant vacuoles (Santos da Silveira et al., 2019). Both IT and IS exhibited negative *t*-value effect for DPPH. Only IT showed a significant positive *t*-value effect for TPA. L–S ratio also had a negative *t*-value effect for DPPH. This meant that, the *t*-value of effect exhibited a decreasing significant influence on DPPH as the L–S ratio increases. This indicated that increasing L–S ratio decreases DPPH, resulting in

Table 1
BBD matrix with experimental design and data for the extraction of CA by SSF technique for one experimental block with *Lactobacillus casei*.

Run	Fermentation parameters (actual and coded values)				Response[c]		
	pH	IT (h)	IS (%)	L–S ratio	CA yield (mg/g)	Fermentation efficiency (%)	DPPH (μmol AA eq/g dry sample)
	X_1	X_2	X_3	X_4			
1	5.00 (-1)	48.00 (+1)	3.00 (0)	0.46 (0)	5.30 ± 0.12	24.97 ± 0.52	73.19 ± 0.27
2	5.00 (-1)	24.00 (0)	5.00 (+1)	0.46 (0)	6.41 ± 0.14	26.44 ± 0.57	73.82 ± 0.35
3	6.00 (0)	24.00 (0)	3.00 (0)	0.46 (0)	5.38 ± 0.07	22.30 ± 0.28	55.90 ± 0.21
4	6.00 (0)	24.00 (0)	1.00 (-1)	0.25 (-1)	5.49 ± 0.06	26.66 ± 0.25	69.62 ± 0.13
5	6.00 (0)	0.00 (-1)	1.00 (-1)	0.46 (0)	5.17 ± 0.08	24.37 ± 0.32	59.77 ± 0.36
6	6.00 (0)	24.00 (0)	3.00 (0)	0.46 (0)	5.40 ± 0.09	22.33 ± 0.36	53.94 ± 0.37
7	6.00 (0)	24.00 (0)	5.00 (+1)	0.25 (-1)	3.85 ± 0.09	23.29 ± 0.39	71.90 ± 0.67
8	7.00 (+1)	24.00 (0)	5.00 (+1)	0.46 (0)	3.92 ± 0.04	25.73 ± 0.18	77.44 ± 0.39
9	5.00 (-1)	24.00 (0)	3.00 (0)	0.25 (-1)	4.70 ± 0.03	28.86 ± 0.11	75.40 ± 0.58
10	7.00 (+1)	24.00 (0)	3.00 (0)	0.25 (-1)	4.84 ± 0.14	24.42 ± 0.60	75.43 ± 0.62
11	5.00 (-1)	24.00 (0)	3.00 (0)	0.67 (+1)	6.28 ± 0.13	26.28 ± 0.56	76.85 ± 0.45
12	6.00 (0)	24.00 (0)	3.00 (0)	0.46 (0)	5.18 ± 0.06	22.10 ± 0.25	53.89 ± 0.08
13	6.00 (0)	48.00 (+1)	5.00 (+1)	0.46 (0)	4.00 ± 0.20	25.61 ± 0.83	71.48 ± 0.47
14	7.00 (+1)	24.00 (0)	3.00 (0)	0.67 (+1)	4.64 ± 0.04	30.59 ± 0.16	72.58 ± 0.22
15	6.00 (0)	0.00 (-1)	5.00 (+1)	0.46 (0)	6.36 ± 0.08	26.61 ± 0.35	60.78 ± 0.62
16	7.00 (+1)	0.00 (-1)	3.00 (0)	0.46 (0)	5.44 ± 0.11	25.04 ± 0.46	67.49 ± 0.51
17	6.00 (0)	0.00 (-1)	3.00 (0)	0.25 (-1)	4.29 ± 0.10	27.93 ± 0.43	72.59 ± 0.63
18	6.00 (0)	48.00 (+1)	1.00 (-1)	0.46 (0)	5.57 ± 0.10	25.26 ± 0.42	57.36 ± 1.16
19	6.00 (0)	0.00 (-1)	3.00 (0)	0.67 (+1)	6.78 ± 0.10	27.40 ± 0.43	53.93 ± 1.56
20	7.00 (+1)	24.00 (0)	1.00 (-1)	0.46 (0)	6.05 ± 0.08	24.43 ± 0.32	63.83 ± 1.21
21	5.00 (-1)	0.00 (-1)	3.00 (0)	0.46 (0)	6.39 ± 0.11	30.08 ± 0.48	62.12 ± 1.17
22	5.00 (-1)	24.00 (0)	1.00 (-1)	0.46 (0)	4.99 ± 0.08	25.07 ± 0.32	71.69 ± 1.17
23	6.00 (0)	24.00 (0)	5.00 (+1)	0.67 (+1)	6.01 ± 0.05	29.12 ± 0.20	77.36 ± 1.14
24	6.00 (0)	48.00 (+1)	3.00 (0)	0.25 (-1)	5.08 ± 0.09	25.22 ± 0.36	59.47 ± 0.70
25	6.00 (0)	24.00 (0)	3.00 (0)	0.46 (0)	5.45 ± 0.03	22.35 ± 0.11	55.72 ± 0.85
26	6.00 (0)	24.00 (0)	3.00 (0)	0.46 (0)	5.19 ± 0.04	23.12 ± 0.19	55.70 ± 0.77
27	6.00 (0)	24.00 (0)	1.00 (-1)	0.67 (+1)	4.77 ± 0.00	23.53 ± 0.00	63.43 ± 0.81
28	7.00 (+1)	48.00 (+1)	3.00 (0)	0.46 (0)	4.62 ± 0.03	29.33 ± 0.11	63.48 ± 0.47
29	6.00 (0)	48.00 (+1)	3.00 (0)	0.67 (+1)	4.13 ± 0.01	29.11 ± 0.04	76.16 ± 0.84

X_1 = pH; X_2 = IT: Incubation time; X_3 = IS: Inoculation size; X_4 = L–S ratio: Liquid-solid ratio.
[C] : Data were mean values (x3).

reduction in antioxidant activity of the LCFHS through oxidation of antioxidant compounds (Kaprasob et al., 2017) dependent on the synergetic and redox interactions among the different compounds present in HS.

The positive *t*-value of effect obtained for IS on TPA indicated that increasing IS, increased TPA, due to the attainment of exponential phase at a short time (Rodríguez de Olmos et al., 2017) with higher activity to release more CA from breaking of the bond between CA and oligosaccharides and/or polysaccharides into free CA through enzymatic degradation (with enzymes produced by *L. casei*) of the oligosaccharides and crude proteins in HS during fermentation (Dulf et al., 2016; Kaprasob et al., 2017; Su et al., 2018). For DPPH, increasing IT and IS decreased the antioxidant activity of LCFHS. This perhaps was as a result of degradation of CA (Heo et al., 2020), therefore, decreasing the actual quantity of CA extracted after fermentation. The statistical importance was determined with a Pareto chart using absolute *t*-value. The limit line from the Pareto chart (Fig. 1), was used to determine the extremely significant (Bonferroni limit line), significant (above *t*-value limit line) and insignificant (below *t*-value limit line) constants of different factors to viscerally establish significant factors (Guo et al., 2018; Zhou et al., 2018). Both IT and IS were extremely significant for Bonferroni limit line for CA yield and fermentation efficiency (Fig. 2**; a and b**). Similar findings were reported. For example, Panesar et al. (2010), in optimizing the process conditions for efficient lactose conversion (in whey) to L(+) lactic acid, found IT and IS to be significant for the process, and achieved maximum lactic acid (33.72 g/L) at IT of 37 °C and IS of 2–4% (v/v). IS, IT, L–S ratio and pH were all extremely significant for DPPH. However, none of the parameters was extremely significant for TPA (Fig. 1c) with the *t*-value of effect below the Bonferroni limit line (used as the threshold for factor selection). Though, IS was significant for TPA, the model for TPA was not significant (*F* value of 1.70). This suggested that TPA was not, probably, a good response indicator for evaluating the effects of the SSF conditions for CA extraction from HS variety hence was not used in further experiments.

The *t*-value limit line (the *t*-value above 2.04) depicted significance of factor for that response (Fig. 1**; a – d)**. In all the responses, *t*-value of temperature was below 2.04 (the *t*-value limit line). The *t*-value of effect of temperature was therefore not significant enough even though it increased. Relative to the IT, IS, pH and L–S ratio, the influence of temperature on the various responses was insignificant. Correspondingly, IT, IS, pH and L–S ratio were thoroughly considered as the significant SSF conditions for further experiments. Nevertheless, temperature, the insignificant factor was also investigated. In fermentation, microorganisms produce enzymes that hydrolyze the substrate to produce specific metabolite. Enzymatic activities are affected by temperature; thus, temperature promotes or inhibits production of a particular metabolite. Best temperature for lactic acid bacteria growth differs between the genus (20–45 °C), however, 30 to 45 ℃ was reported optimal for *L. casei* (Panesar et al., 2010; Qi and Yao, 2007). Regulation of temperature is therefore important for high efficiency of *L. casei* to produce desired result. The results showed that a relatively mid temperature (40 °C) might help in increasing the interaction between HS and *L. casei* and hence, enhance responses.

3.2. Fitting models for extraction of CA from HS variety under SSF method

From the BBD analysis, the results obtained showed that pH (X_1), IT (X_2), IS (X_3) and L–S ratio (X_4) significantly influenced the DPPH, the fermentation efficiency of *L. casei* and the yield of CA extracted from the HS variety under SSF technique (Table 1). In finding an appropriate model for the CA yield, fermentation efficiency and DPPH (dependent variables), the results revealed the quadratic models with R^2 values above 99.30 % indicatory of less than 1% (only 0.70 %) of the total

Table 2
ANOVA, regression analysis and optimal conditions for CA extraction from HS variety by SSF with *L. casei*.

Source	CA yield (mg/g)		Fermentation efficiency (%)		DPPH (μmol AA eq/g dry sample)	
	F-value	*p*-value	*F*-value	*p*-value	*F*-value	*p*-value
Model	183.50	< 0.0001***	155.98	< 0.0001***	377.32	< 0.0001***
Linear						
X_1 = A: pH	251.28	< 0.0001***	5.00	0.0422*	37.48	< 0.0001***
X_2 = B: IT	396.77	< 0.0001***	3.99	0.0656 ^{NS}	136.43	< 0.0001***
X_3 = C: IS	26.83	0.0001***	59.93	< 0.0001***	505.46	< 0.0001***
X_4 = D: L–S ratio	229.72	< 0.0001***	99.74	< 0.0001***	3.83	0.0705 ^{NS}
Interactions						
AB	2.64	0.1263 ^{NS}	283.92	< 0.0001***	155.57	< 0.0001***
AC	456.89	< 0.0001***	0.016	0.9019 ^{NS}	90.16	< 0.0001***
AD	114.87	< 0.0001***	246.01	< 0.0001***	12.65	0.0032*
BC	276.17	< 0.0001***	11.48	0.0044**	117.58	< 0.0001***
BD	429.01	< 0.0001***	62.77	< 0.0001***	854.89	< 0.0001***
CD	300.70	< 0.0001***	257.96	< 0.0001***	92.85	< 0.0001***
Quadratic						
A^2	5.41	0.0356*	505.37	< 0.0001***	1963.64	< 0.0001***
B^2	0.36	0.3600 ^{NS}	489.59	< 0.0001***	20.72	0.0005**
C^2	2.16	0.1638 ^{NS}	27.29	0.0001***	674.18	< 0.0001***
D^2	65.64	< 0.0001***	567.20	< 0.0001***	1582.76	< 0.0001***
Fitting statistics						
Lack of fit	0.21	0.9796 ^{NS}	0.31	0.9417 ^{NS}	0.091	0.9989 ^{NS}
R^2	0.9946		0.9936		0.9974	
Adjusted R^2	0.9892		0.9873		0.9947	
Predicted R^2	0.9837		0.9785		0.9938	
Adeq. Precision	49.827		39.291		53.133	
C.V. %	1.590		1.08		0.91	
Standard Dev.	0.083		0.28		0.60	

Optimization equations

$$CA\ yield\ (mg/g) = 5.32 - 0.38X_1 - 0.48X_2 - 0.12X_3 + 0.36X_4 + 0.067X_1X_2 - 0.89X_1X_3 - 0.45X_1X_4 - 0.69X_2X_3 - 0.86X_2X_4 + 0.72X_3X_4 + 0.076{X_1}^2 + 0.02{X_2}^2 - 0.048{X_3}^2 - 0.26{X_4}^2$$

$$Fermentation\ efficiency\ (\%) = 22.44 - 0.18X_1 - 0.16X_2 + 0.62X_3 + 0.8X_4 + 2.35X_1X_2 - 0.018X_1X_3 + 2.19X_1X_4 - 0.47X_2X_3 + 1.11X_2X_4 + 2.24X_3X_4 + 2.46{X_1}^2 + 2.42{X_2}^2 + 0.57{X_3}^2 + 2.61{X_4}^2$$

$$DPPH\ (\mu mol\ AA\ eq/g\ dry\ sample) = 55.03 - 1.07X_1 + 2.04X_2 + 3.92X_3 - 0.34X_4 - 3.77X_1X_2 + 2.87X_1X_3 - 1.07X_1X_4 + 3.28X_2X_3 + 8.84X_2X_4 + 2.91X_3X_4 + 10.52{X_1}^2 + 1.08{X_2}^2 + 6.16{X_3}^2 + 9.44{X_4}^2$$

*, ** and *** denote significance at $p < 0.05$, $p < 0.01$ and $p < 0.001$ respectively while ^{NS} denotes not significant.

factors of the respective responses were not explained by their quadratic models (Table 2). Likewise, their *adjusted* R^2 values above 98.70 % revealed elimination of insignificant terms in their models and signified an excellent correlation between the independent variables (Khan and Tripathi, 2011; Mintah et al., 2020). Accordingly, their lack of fits (*p*-value = 97.96 %, 94.17 %, 99.89 % for CA yield, fermentation efficiency and DPPH respectively), indicated the credibility and good fitness of their models with CA yield ranged from 3.85 ± 0.09–6.78 ± 0.10 mg/g, fermentation efficiency from 22.10 ± 0.25–30.59 ± 0.16 % and DPPH from 53.89 ± 0.08–77.44 ± 0.39 μmol AA eq/g dry sample. Relative to their pure errors and fitness of their models, their lack of fits were insignificant, an indication of sufficient models (Mintah et al., 2020). The analysis of variance (ANOVA) results indicated highly significant ($p < 0.0001$) quadratic models. Consequently, indicative of their ability to appropriately explain real relationship between the respective response variables and their experimental factors (Dabbour et al., 2018; Mintah et al., 2020). Their coefficient of variation (CV) values less than 1.60 confirmed the reliability and reproducibility of the experiments for the response variables (Mintah et al., 2020). Furthermore, the results established the accuracy of the experimental models. The BBD data therefore fitted well and was an excellent adequacy second-order polynomial regression equation model for the responses (Table 1).

3.3. Effect of variables on CA yield of HS variety

Table 1 displayed the BBD used to predict CA yield from HS variety. It showed that pH (X_1), IT (X_2), IS (X_3) and L–S ratio (X_4) had significant influence on CA yield extracted from the HS variety. To eliminate the insignificant variables, ANOVA was used, which gave X_1, X_2, X_3, X_4, X_1X_3, X_1X_4, X_2X_3, X_2X_4, X_3X_4 X_1^2 and X_4^2 as the important variables. The simplified model showed highly significant effect ($p < 0.0001$) of the four SSF parameters on CA yield by the 2nd order polynomial regression equation as follows:

$$CA\ (mg/g) = 5.32 - 0.38X_1 - 0.48X_2 - 0.12X_3 + 0.36X_4 - 0.89X_1X_3 - 0.45X_1X_4 - 0.69X_2X_3 - 0.86X_2X_4 + 0.72X_3X_4 + 0.076{X_1}^2 - 0.26{X_4}^2 \quad (6)$$

Display of the relationship between factor and its dependent variables is the indispensable function of RSM (Bi et al., 2014; Guo et al., 2018). This was evident by keeping one parameter at zero-level (Fig. 2**; a – f**). All the factors (pH, IT, IS and L–S ratio) significantly contributed to the linear model. Except the quadratic effects of X_2 and X_3 which were not significant, that of X_1 and X_4 significantly contributed to the quadratic model. Also, the interactive effects of all the factors with the exception of pH and IT (X_1X_2) were significant. This information might be relevant to the industry regarding influence or importance of two factor combinations on CA yield in SSF extraction processes. The maximum CA yield (6.78 ± 0.10 mg/g) was obtained at pH = 6.00, IT = 0.00 h, IS = 3.00 % and L–S ratio = 0.67 whilst the minimum CA yield (3.85 ± 0.09 mg/g) was at pH = 6.00, IT = 24.00 h, IS = 5.00 % and L–S ratio = 0.25. The high CA yield obtained by this SSF technique was in agreement with report of Rodríguez de Olmos et al. (2017), that SSF process gives higher yield of products. The RSM also confirmed that when pH, IT, and IS values were fixed, L–S ratio had a positive effect on CA yield (increased L–S ratio resulted in increased CA yield). The reverse was obtained for the rest of the factors. That is, for fixed values of IT, IS and L–S ratio, pH had a negative effect on CA yield and same

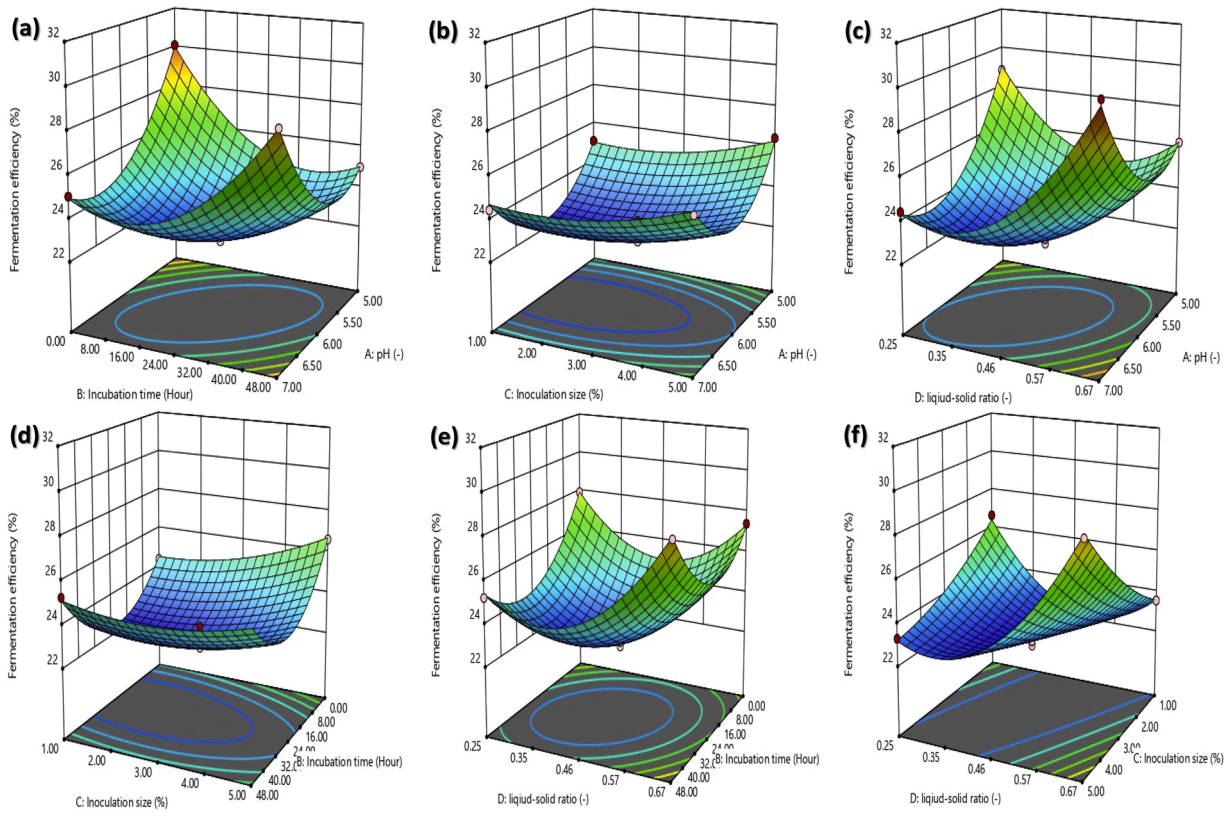

Fig. 3. Response surface and contour plots of interactive effects of pH, incubation time, inoculation size and liquid-solid ratio on the fermentation efficiency of HS variety.

observations obtained for IT and IS when the values of the other factors were held fixed respectively. The increase of L–S ratio, IS and IT and decreasing of pH increased the CA yield by increasing the proliferation and efficiency of *L. casei* for significant increase of CA extraction. The negative effect of pH, IT and IS on CA yield and the opposite shown by L–S ratio was displayed by the perturbation plot. Perturbation plot confirmed that an increase in L–S ratio resulted in a gradual rise of CA yield and echoed RSM. Desirability curve was used to obtained the optimum CA yield (8.80 ± 0.08 mg/g). Thus, CA yield of 8.72–8.89 mg/g was selected as the most desirable.

3.4. Effect of variables on fermentation efficiency of L. casei on HS variety

The effect of the quadratic (RSM) model, variables and their interactions on fermentation efficiency of *L. casei* (Fig. 3; **a – f**) was illustrated by ANOVA. The fermentation efficiency values were significantly influenced by X_1, X_3, X_4, X_1X_2, X_1X_4, X_2X_3, X_2X_4, X_3X_4, X_1^2, X_2^2, X_3^2 and X_4^2. Consequently, the model was reduced to:

$$\begin{aligned} \textit{Fermentation efficiency}\ (\%) = {} & 22.44 - 0.18X_1 + 0.62X_3 + 0.8X_4 + 2.35X_1X_2 \\ & + 2.19X_1X_4 - 0.47X_2X_3 + 1.11X_2X_4 \\ & + 2.24X_3X_4 + 2.46{X_1}^2 + 2.42{X_2}^2 + 0.57{X_3}^2 \\ & + 2.61{X_4}^2 \end{aligned} \quad (7)$$

The credibility of this model was confirmed by the R^2 value (99.36 %) and the lack-of-fit test (94.17 %) (Table 2). As evident by the results, pH and IT (X_1X_2), pH and L–S ratio (X_1X_4), IT and IS (X_2X_3), IT and L–S ratio (X_2X_4) and IS and L–S ratio (X_3X_4) contributed significantly to the interactive effect. A synergetic effect on fermentation efficiency was attained with increasing of X_2 and decreasing of X_3. The results also revealed significant contribution of X_1, X_3 and X_4 to the linear equation.

The contour and 3-D response surface (RS) plots for fermentation efficiency (Fig. 3; **a – f**) indicated that the fermentation efficiency first decreased gradually with increasing pH, IT and L–S ratio to a threshold level, then increased steadily as the factors increased beyond this level. This could be that the conditions for growth of *L. casei* was not favourable when pH, IT and L–S ratio were below the threshold level. However, as the factors increased beyond the threshold level, the optimum conditions (especially L–S ratio) for proliferation of *L. casei* were attained and their activity increased leading to the high fermentation efficiency obtained after the threshold level. This is in agreement with the report of Guo et al. (2018), which found that increasing L–S ratio increases nutrient substance in medium for microbial cells utilization and enhanced activity. Increased fermentation efficiency (22.10 ± 0.25–30.59 ± 0.16 %) was obtained among the different variables. A negative effect of pH and IT and a positive effect of L–S ratio and IS on fermentation efficiency was revealed by the perturbation plot. The curve of IS (curve C) from the perturbation plot, exhibited a slightly steeper continual increase relative to the rest (curves A, B and D). The results indicated that the fermentation efficiency was noticeably influenced by IS. This result was in similitude with previous studies (Rodríguez de Olmos et al., 2017), which found exponential growth phase of lactobacilli strains with higher efficiency at a shorter SSF hours when inoculum concentration or size was increased. Thus, IS and L–S ratio were two crucial factors for the fermentation efficiency of *L. casei*.

3.5. Effect of variables on DPPH of HS variety

The BBD used for the prediction of DPPH of HS variety was depicted in Table 1. The significant variables that had effects on DPPH were X_1, X_2, X_3, X_1X_2, X_1X_3, X_1X_4, X_2X_3, X_2X_4, X_3X_4, X_1^2, X_2^2, X_3^2 and X_4^2, obtained from the ANOVA results. Accordingly, the simplified model was:

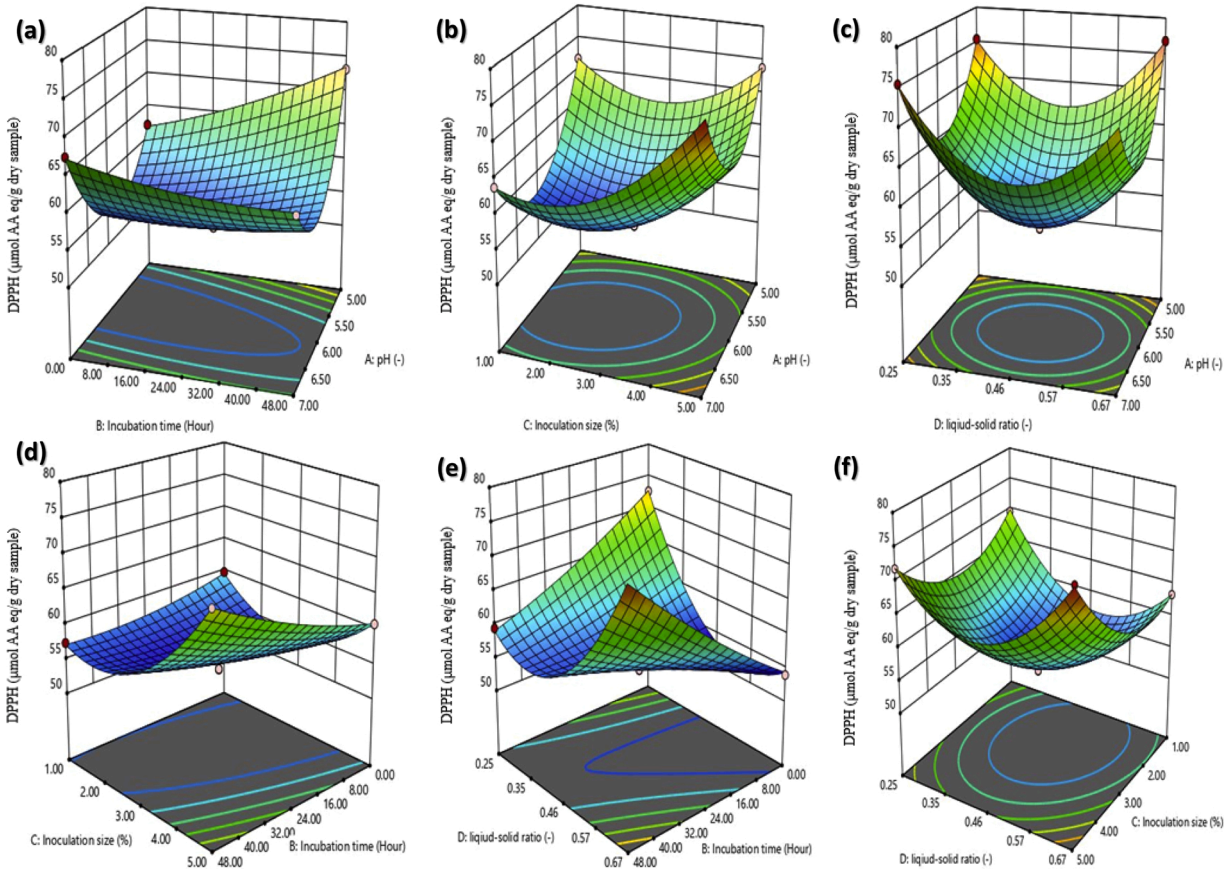

Fig. 4. Response surface and contour plots of interactive effects of pH, incubation time, inoculation size and liquid-solid ratio on the DPPH of HS variety.

$$DPPH\ (\mu mol\ AA\ eq/g\ dry\ sample) = 55.03 - 1.07X_1 + 2.04X_2 + 3.92X_3 - 3.77X_1X_2 + 2.87X_1X_3 - 1.07X_1X_4 + 3.28X_2X_3 + 8.84X_2X_4 + 2.91X_3X_4 + 10.52{X_1}^2 + 1.08{X_2}^2 + 6.16{X_3}^2 + 9.44{X_4}^2 \quad (8)$$

The model credibility was justified by the R^2 value (99.74 %) and a lack-of-fit test of 99.89 % (Table 2). The 3-D RS and contour plots (Fig. 4; **a – f**) were developed to examine the interaction between the factors as well as to determine the ideal conditions to achieve a maximum DPPH. The interactive effect of all the factors was significant. DPPH increased with increased IT (Fig. 4; **e**) while L–S ratio was fixed. Similar observation was obtained when IS was held at zero (0-level) and IT increased. This indicated that IT had a more noticeable effect on DPPH than the other variables. The perturbation plot confirmed it. Dulf et al. (2016) reported that SSF increases total phenolic compounds which contributes to antioxidant activity. They found increased total phenolics under SSF with *R. oligosporus* (greater than 30 %) and *A. niger* (greater than 21 %). Soybean is a good source of antioxidant comprising of isoflavones, genistein, daidzein, flavonoids and phenolic acids (Nam et al., 2014; Zamindar et al., 2017). However, Nam et al. (2014) stated that the antioxidant activity of soybean correlates with total phenolics and isoflavones positively. The observed increase in DPPH with respect to IT might be due to enzymatic hydrolysis (with carbohydrate degrading enzymes produced by *L. casei*) of phenolic conjugates (bonded to sugar moieties, organic acids, amines and lipids) to increase the concentration of free phenolics during SSF (Dulf et al., 2016). The fermentation of the HS variety with *L. casei* using SSF technology could enhance the recovery of valuable hydro- and lipophilic compounds positively (Dulf et al., 2016), liberating free polyphenols and increasing the antioxidant activity as the IT and IS increased. Rodríguez de Olmos et al. (2017) reported similar results.

3.6. Optimization and verification of the predictive model

The main goal of this method was to estimate the levels of independent variables to give maximum CA yield, fermentation efficiency and DPPH values. The responses (CA yield, fermentation efficiency and DPPH) were optimized with Design Expert version 11.0.5.0. Desirability function method was applied to optimize the selected SSF conditions (pH, IT, IS and L–S ratio) with the response parameters set to maximum. According to Granato and Ares (2014), desirability function sets a score (ranging from 0 to 1) to responses and selects parameter settings that increase the score for the optimization of conglomerate responses. The optimum SSF conditions for CA extraction from HS variety using *L. casei* were determined to obtain the maximum CA yield, fermentation efficiency and DPPH. The predicted optimum SSF conditions were pH = 5.02, IT = 11.52 h, IS = 5.00 % and L–S ratio = 0.67 from the desirability function settings and the maximum CA yield, fermentation efficiency and DPPH achieved were 8.80 ± 0.08 mg/g, 31.29 ± 0.28 % and 77.45 ± 0.60 μmol AA eq/g dry sample respectively. The desirability of the results obtained was 1.00. Verification tests were performed with the obtained SSF conditions to investigate and verify the reliability of the results. Both the relative errors and the residual standard errors obtained for the predicted and experimental values were less than 5% (Boateng et al., 2020; Boateng and Yang, 2021). This showed that the model was adequate and precise (Granato and Ares, 2014).

3.7. CA yield and antioxidant activity of raw and fermented HS variety

The results of the optimized SSF conditions for CA extraction from

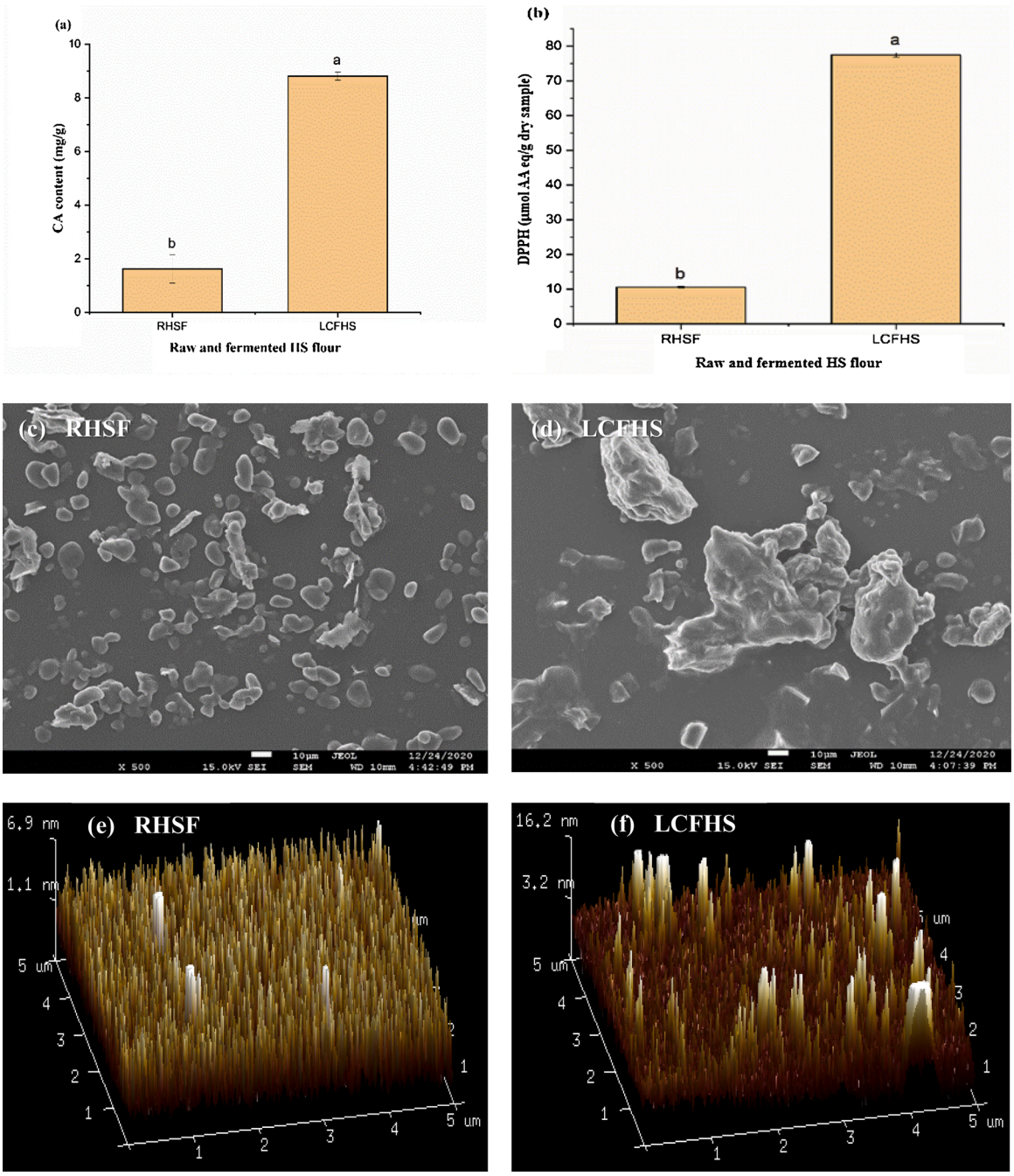

Fig. 5. CA (a) and DPPH (b) contents, SEM and AFM micrographs of raw HS flour (RHSF) and *Lactobacillus casei* fermented HS (LCFHS).

LCFHS sample and direct extraction of CA from RHSF sample were shown in Fig. 5 (a and b). Noticeable, significant ($p < 0.05$) improvement of CA yield and antioxidant activity measured by DPPH method was obtained for the SSF process. The CA yield and antioxidant activity obtained by the direct extraction process from the RHSF sample were 1.62 ± 0.53 mg/g and 10.57 ± 0.21 μmol AA eq/g dry sample respectively. Whilst the CA yield and antioxidant activity of the LCFHS under the optimized SSF conditions were 8.80 ± 0.08 mg/g and 77.45 ± 0.60 μmol AA eq/g dry sample respectively. Relative to the direct extraction process, the CA yield and the DPPH obtained for the optimized SSF conditions increased by 5.43-fold (with extraction efficiency of 550 %) and 7.33-fold respectively. These results agreed with that of Rodríguez de Olmos et al. (2017) and Dulf et al. (2016). Furthermore, the extraction efficiency (550 %) obtained in this study was higher than that (6.70 %) of Li et al. (2005) obtained in ultrasound aided extraction of CA from *Eucommia ulmodies* Oliv, and 400 % reported by Santos da Silveira et al. (2019) for SSF of coffee pulp. In addition, the liquid medium (water) used for the extraction is less expensive, making the application of the process cost-effective at the pilot- or industrial-scale level. As a result, the study outcome proved that the optimized SSF conditions are very useful for application in the food, pharmaceutical and cosmetic industries for high CA yield production with improved antioxidant activity.

3.8. Effect of SSF on the morphology of HS variety

SEM and AFM analyses were performed to study the changes that occurred in the microstructure (pellets size, cell size, shape, density and homogeneity) of the RHSF after SSF with *L. casei* at the optimized conditions. Fig. 5**; c and d** showed the micrographs of RHSF and LCFHS

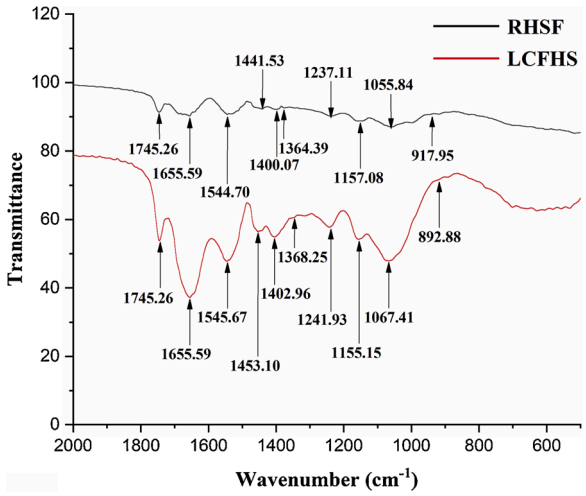

Fig. 6. FTIR spectra of raw HS flour (RHSF) and *L. casei* fermented HS (LCFHS).

samples. The results revealed the effect of the optimized SSF conditions on the morphology of the HS variety. The RHSF sample exhibited discrete and aggregated spherical and/or irregular granules with smaller sizes and smooth surfaces shown in Fig. 5**; c.** However, in the LCFHS micrograph **(**Fig. 5**; d)**, agglomerated fragments that were irregular in shape and size with a part scattered were observed, possibly due to the SSF process affecting microstructure of the HS. The micrograph of LCFHS sample was significantly different from that of RHSF sample. The results were consistent with that of Sulieman et al. (2019) which found polysaccharide flour fermented by *Agaricus bisporus* with agglomerated fragments that were irregular in shape and size and Liu et al. (2016) who reported agglomerated particles with a part scattered and irregular shapes of polysaccharide from cultivated fruit bodies and mycelium of *Cordyceps militaris*. SEM images of LCFHS sample enlarged to ×1000 times showed that the surface topography was rough with pits in the chain structure. Furthermore, the microstructures of LCFHS sample **(**Fig. 5**; d)** were looser and more characterized by continuous structures with irregular granules. This resulted from the breakdown of cell walls and bonds between molecules, shown by a number of empty areas compared to RHSF sample **(**Fig. 5**; c)**. Thus, led to the release of more free CA, hence the observed increase obtained in the LCFHS sample (Santos da Silveira et al., 2019; Su et al., 2018). Overall, factors which influenced the morphological properties of LCFHS sample were granule sizes and shape, which may be due to the fermentation process. The change in the structure of RHSF and LCFHS samples were further confirmed with AFM analysis. AFM topographic images give more observations such as 3-D height, distribution/size, and number/shape of particles of molecules. The topography of RHSF exhibited a regular reticulate structure. (Fig. 5**; e**). While in the LCFHS, loosed non-reticulate structure and irregular large-sized particles was observed. (Figs. 5**; f**). Furthermore, the height and number of LCFHS particles reduced compared to RHSF sample. The particles of LCFHS also showed scattered and partially destroyed micropores. The results showed that SSF exhibited significant effect on the structural alterations of the HS variety.

3.9. Effect of SSF on FTIR of HS variety

The FTIR spectra for the RHSF and LCFHS samples investigated were presented in Fig. 6. Spectral trend similarities and peak shifts between both samples were observed. The changes or shifts in cellulose, hemicellulose and lignin peak positions were used to analyze the extent of structural changes in the cell wall of the RHSF and LCFHS samples examined. The glucose sugar polymers, cellulose and hemicellulose absorption peak position of RHSF sample at approximately 918 cm^{-1} was changed in LCFHS sample to a band position of approximately 893 cm^{-1} owing to β-glycosidic linkages (Fakayode et al., 2020). The above large change in the peak locations observed was significant and revealed that the glucose sugar polymers, cellulose and hemicellulose structures of the cell wall of the HS variety were broken-down after the SSF. This probably led to the release of more, free CA contributing to the high CA content mentioned in section 3.7. Both samples had peaks at approximately 1056 and 1067 cm^{-1} respectively representing the C—O stretching vibration of the cellulose, hemicellulose, and lignin of the cell wall of HS variety. Absorption peaks at approximately 1157 and 1155 cm^{-1} for RHSF and LCFHS samples respectively were characteristic of C—O—C asymmetrical-stretching vibration of cellulose and hemicellulose (Li et al., 2018). The lignin absorption peak position in RHSF sample at approximately 1237 cm^{-1} was changed to approximately 1242 cm^{-1} in LCFHS sample, typical of C—O—C alkyl aryl ether bond (Loow et al., 2017). Also, there were small but noticeable absorption peaks at approximately 1364 cm^{-1} for RHSF sample and 1368 cm^{-1} for LCFHS sample attributed to CH_3 symmetrical angular vibration in cellulose and hemicellulose (Li et al., 2018). The band peaks observed at approximately 1400 and 1442 cm^{-1} (for RHSF sample) and 1402 and 1453 cm^{-1} (for LCFHS sample) were due to the bending vibrations of the symmetrical CH_2 groups in cellulose (Loow et al., 2017). In comparison with the RHSF sample, the slight shift of its peak at approximately 1545 to 1546 cm^{-1} (in LCFHS sample) after the fermentation process signified the aromatic skeletal C═C vibration in lignin aromatic ring. This showed that the SSF release significant amounts of phenolics (Loow et al., 2017). The large transmittance peak at approximately 1656 cm^{-1} for both samples were attributed to COOH groups stretching vibration in lignin, cellulose and hemicellulose aromatic ring (Li et al., 2018). Similarly, same peaks position at approximately 1745 cm^{-1} were obtained for both samples, depicting the presence of C═O stretching vibration of ester groups in hemicellulose (Loow and Wu, 2018). The change in the locations of lignin, cellulose and hemicellulose between the samples indicated structural alterations in the cell wall of the HS variety. These alterations were attributed to the effect of SSF, which caused breakage in the interactions between the lignin, cellulose and hemicellulose sequences and the other linkage bonds in the cell wall structure of the HS variety.

4. Conclusion

A two-step optimization process of SSF was established through HS engineering with *L. casei* to extract CA with high yield, fermentation efficiency, and antioxidant activity (DPPH). The LCFHS sample displayed higher CA yield (5.43-fold) and DPPH (7.33-fold) than RHSF sample. The experimental data compared very well with the predicted values; suggestive that the selected RSM (BBD) model was successfully applied for SSF of HS variety to extract high CA yield with improved antioxidant activity. The AFM, FTIR and SEM results established the effectiveness of the optimized SSF conditions on the breakdown of the cell wall of HS. Desirability function was 1.00, depicting the adequacy, precision and acceptability of the model. The use of HS for CA extraction therefore competes with the best dietary sources of CA, opening up a way for efficient commercial application of HS for CA extraction.

CRediT authorship contribution statement

Nelson Dzidzorgbe Kwaku Akpabli-Tsigbe: Conceptualization, Methodology, Software, Validation, Formal analysis, Investigation, Data curation, Writing - original draft, Writing - review & editing, Visualization. **Yongkun Ma:** Supervision, Resources, Project administration, Funding acquisition. **John-Nelson Ekumah:** Investigation. **Juliet Osabutey:** Writing - review & editing. **Jie Hu:** Investigation. **Manqing Xu:** Investigation. **Nana Adwoa Nkuma Johnson:** Investigation. **Janet Quaisie:** Investigation.

Declaration of Competing Interest

The authors report no declarations of interest.

Acknowledgment

The authors are grateful for the support provided by the Zhenjiang Key Research and Development Program (Modern Agriculture) [grant number NY2020020].

Appendix A. Supplementary data

Supplementary material related to this article can be found, in the online version, at doi:https://doi.org/10.1016/j.indcrop.2021.113565.

References

Adane, T.D., Yoseph, A.A., Kusse, G.G., 2019. Determination of chlorogenic acid content in beans and leaves of *Coffea arabica* using UV/Vis spectrometer. African J. Pure Appl. Chem. 13, 58–63. https://doi.org/10.5897/ajpac2018.0780.

Alves Filho, E.G., Sousa, V.M., Rodrigues, S., de Brito, E.S., Fernandes, F.A.N., 2020. Green ultrasound-assisted extraction of chlorogenic acids from sweet potato peels and sonochemical hydrolysis of caffeoylquinic acids derivatives. Ultrason. Sonochem. 63, 104911 https://doi.org/10.1016/j.ultsonch.2019.104911.

Bi, J., Chen, Q., Zhou, Y., Liu, X., Wu, X., Chen, R., 2014. Optimization of short- and medium-wave infrared drying and quality evaluation of jujube powder. Food Bioprocess Technol. 7, 2375–2387. https://doi.org/10.1007/s11947-013-1245-y.

Boateng, I.D., Yang, X.-M., 2021. Process optimization of intermediate-wave infrared drying: screening by Plackett–Burman; comparison of Box-Behnken and central composite design and evaluation: a case study. Ind. Crops Prod. 162, 113287 https://doi.org/10.1016/j.indcrop.2021.113287.

Boateng, I.D., Yang, X., Li, Y., 2020. Optimization of infrared-drying parameters for *Ginkgo biloba* L. seed and evaluation of product quality and bioactivity. Ind. Crop. Prod. 160, 1–10. https://doi.org/10.1016/j.indcrop.2020.113108.

Chen, K.I., Erh, M.H., Su, N.W., Liu, W.H., Chou, C.C., Cheng, K.C., 2012. Soyfoods and soybean products: from traditional use to modern applications. Appl. Microbiol. Biotechnol. 96, 9–22. https://doi.org/10.1007/s00253-012-4330-7.

Cho, A., Jeon, S., Kim, M., Yeo, J., Seo, K., Choi, M., Lee, M., 2010. Chlorogenic acid exhibits anti-obesity property and improves lipid metabolism in high-fat diet-induced-obese mice. Food Chem. Toxicol. 48, 937–943. https://doi.org/10.1016/j.fct.2010.01.003.

Correa Deza, M.A., Rodríguez de Olmos, A., Garro, M.S., 2019. Solid state fermentation to obtain vegetable products bio-enriched with isoflavone aglycones using lactic cultures. Rev. Argent. Microbiol. 51, 201–207. https://doi.org/10.1016/j.ram.2018.04.006.

Dabbour, M., He, R., Ma, H., Musa, A., 2018. Optimization of ultrasound assisted extraction of protein from sunflower meal and its physicochemical and functional properties. J. Food Process Eng. 41, 1–11. https://doi.org/10.1111/jfpe.12799.

Dabbour, M., Alenyorege, E.A., Mintah, B., He, R., Jiang, H., Ma, H., 2020. Proteolysis kinetics and structural characterization of ultrasonic pretreated sunflower protein. Process Biochem. 94, 198–206. https://doi.org/10.1016/j.procbio.2020.04.018.

Dulf, F.V., Vodnar, D.C., Socaciu, C., 2016. Effects of solid-state fermentation with two filamentous fungi on the total phenolic contents, flavonoids, antioxidant activities and lipid fractions of plum fruit (*Prunus domestica* L.) by-products. Food Chem. 209, 27–36. https://doi.org/10.1016/j.foodchem.2016.04.016.

Fakayode, O.A., Aboagarib, E.A.A., Yan, D., Li, M., Wahia, H., Mustapha, A.T., Zhou, C., Ma, H., 2020. Novel two-pot approach ultrasonication and deep eutectic solvent pretreatments for watermelon rind delignification: parametric screening and optimization via response surface methodology. Energy 203, 117872. https://doi.org/10.1016/j.energy.2020.117872.

Feng, L., Xie, Y., Peng, C., Liu, Y., Wang, H., 2018. A novel antidiabetic food produced via solid-state fermentation of Tartary buckwheat by *L. plantarum* TK9 and *L. paracasei* TK1501. Food Technol. Biotechnol. 56, 373–380. https://doi.org/10.17113/ftb.56.03.18.5540.

Granato, D., Ares, G., 2014. Mathematical and Statistical Methods in Food Science and Technology, first. edit. John Wiley & Sons, Ltd., West Sussex, UK https://doi.org/10.1002/9781118434635.

Guo, N., Song, X.R., Kou, P., Zang, Y.P., Jiao, J., Efferth, T., Liu, Z.M., Fu, Y.J., 2018. Optimization of fermentation parameters with magnetically immobilized *Bacillus natto* on Ginkgo seeds and evaluation of bioactivity and safety. LWT - Food Sci. Technol. 97, 172–179. https://doi.org/10.1016/j.lwt.2018.06.046.

Haida, Z., Hakiman, M., 2019. A comprehensive review on the determination of enzymatic assay and nonenzymatic antioxidant activities. Food Sci. Nutr. 7, 1555–1563. https://doi.org/10.1002/fsn3.1012.

Heo, J., Adhikari, K., Choi, K.S., Lee, J., 2020. Analysis of caffeine, chlorogenic acid, trigonelline, and volatile compounds in cold brew coffee using high-performance liquid chromatography and solid-phase microextraction—gas chromatography-mass spectrometry. Foods 9, 1–2. https://doi.org/10.3390/foods9121746.

Ji, L., Jiang, P., Lu, B., Sheng, Y., Wang, X., Wang, Z., 2013. Chlorogenic acid, a dietary polyphenol, protects acetaminophen-induced liver injury and its mechanism. J. Nutr. Biochem. 24, 1911–1919. https://doi.org/10.1016/j.jnutbio.2013.05.007.

Kaprasob, R., Kerdchoechuen, O., Laohakunjit, N., Sarkar, D., Shetty, K., 2017. Fermentation-based biotransformation of bioactive phenolics and volatile compounds from cashew apple juice by select lactic acid bacteria. Process Biochem. 59, 141–149. https://doi.org/10.1016/j.procbio.2017.05.019.

Karlapudi, A.P., Krupanidhi, S., Reddy, E.R., Indira, M., Bobby, M.N., Venkateswarulu, T. C., 2018. Plackett-Burman design for screening of process components and their effects on production of lactase by newly isolated *Bacillus* sp. VUVD101 strain from Dairy effluent. Beni-Suef Univ. J. Basic Appl. Sci. 7, 543–546. https://doi.org/10.1016/j.bjbas.2018.06.006.

Khan, M., Tripathi, C.K.M., 2011. Optimization of fermentation parameters for maximization of actinomycin D production. J. Chem. Pharm. Res. 3, 281–289.

Kwaw, E., Ma, Y., Tchabo, W., Apaliya, M.T., Xiao, L., Li, X., Hu, M., 2017. Effect of fermentation parameters and their optimization on the phytochemical properties of lactic-acid-fermented mulberry juice. J. Food Meas. Charact. 11, 1462–1473. https://doi.org/10.1007/s11694-017-9525-2.

Li, H., Chen, B., Yao, S., 2005. Application of ultrasonic technique for extracting chlorogenic acid from *Eucommia ulmodies* Oliv. (*E. ulmodies*). Ultrason. Sonochem. 12, 295–300. https://doi.org/10.1016/j.ultsonch.2004.01.033.

Li, X., Wei, Y., Xu, J., Xu, N., He, Y., 2018. Quantitative visualization of lignocellulose components in transverse sections of moso bamboo based on ftir macro- and micro-spectroscopy coupled with chemometrics. Biotechnol. Biofuels 11, 1–16. https://doi.org/10.1186/s13068-018-1251-4.

Li, S., Jin, Z., Hu, D., Yang, W., Yan, Y., Nie, X., Lin, J., Zhang, Q., Gai, D., Ji, Y., Chen, X., 2020. Effect of solid-state fermentation with *Lactobacillus casei* on the nutritional value, isoflavones, phenolic acids and antioxidant activity of whole soybean flour. LWT - Food Sci. Technol. 125, 109264 https://doi.org/10.1016/j.lwt.2020.109264.

Liu, X.-C., Zhu, Z.-Y., Tang, Y.-L., Wang, M.-F., Wang, Z., Liu, A.-J., Zhang, Y.-M., 2016. Structural properties of polysaccharides from cultivated fruit bodies and mycelium of *Cordyceps militaris*. Carbohydr. Polym. 142, 63–72. https://doi.org/10.1016/j.carbpol.2016.01.040.

Loow, Y.-L., Wu, T.Y., 2018. Transformation of oil palm fronds into pentose sugars using copper (II) sulfate pentahydrate with the assistance of chemical additive. J. Environ. Manage. 216, 192–203. https://doi.org/10.1016/j.jenvman.2017.04.084.

Loow, Y.-L., Wu, T.Y., Lim, Y.S., Tan, K.A., Siow, L.F., Md. Jahim, J., Mohammad, A.W., 2017. Improvement of xylose recovery from the stalks of oil palm fronds using inorganic salt and oxidative agent. Energy Convers. Manage. 138, 248–260. https://doi.org/10.1016/j.enconman.2016.12.015.

Magro, A.E.A., Silva, L.C., Rasera, G.B., de Castro, R.J.S., 2019. Solid-state fermentation as an efficient strategy for the biotransformation of lentils: enhancing their antioxidant and antidiabetic potentials. Bioresour. Bioprocess. 6. https://doi.org/10.1186/s40643-019-0273-5.

Martins, S., Mussatto, S.I., Martínez-Avila, G., Montañez-Saenz, J., Aguilar, C.N., Teixeira, J.A., 2011. Bioactive phenolic compounds: production and extraction by solid-state fermentation. A review. Biotechnol. Adv. 29, 365–373. https://doi.org/10.1016/j.biotechadv.2011.01.008.

Miladinovic, J., Malen, D., Cvejic, J., 2012. Polyphenol content and antioxidant properties of colored soybean seeds from central Europe Djordje. J. Med. Food 15, 89–95. https://doi.org/10.1089/jmf.2010.0329.

Mintah, B.K., He, R., Agyekum, A.A., Dabbour, M., Golly, M.K., Ma, H., 2020. Edible insect protein for food applications: extraction, composition, and functional properties. J. Food Process Eng. 43, 1–12. https://doi.org/10.1111/jfpe.13362.

Musa, A., Gasmalla, M.A.A., Ma, H., Sarpong, F., Wali, A., Awad, F.N., Duan, Y., 2019. Effect of a multi-frequency counter-current S-type ultrasound pretreatment on the defatted corn germ protein: enzymatic hydrolysis, ACE inhibitory activity and structural characterization. Food Funct. 10, 6020–6029. https://doi.org/10.1039/c9fo01531k.

Nam, J.-H., Kang, S.-W., Hong, S.-Y., Kim, S.-J., Jin, Y.-I., Kim, H.-S., Yoon, Y.-H., Jeong, J.-C., Pan, C.-H., Um, B.-H., Nho, C.-W., Ok, H.-C., 2014. Analysis of the phenolic content and antioxidant activities of soybean extracts from different regions and cultivars. Korean J. Plant Resour. 27, 610–621. https://doi.org/10.7732/kjpr.2014.27.6.610.

Panesar, P.S., Kennedy, J.F., Knill, C.J., Kosseva, M., 2010. Production of l(+) lactic acid using *Lactobacillus casei* from whey. Braz. Arch. Biol. Technol. 53, 219–226. https://doi.org/10.1590/S1516-89132010000100027.

Plackett, L., Burman, J.P., 1946. The design of optimum multifactorial experiments. Biometrika 33, 305–325.

Pratt, D.E., Birac, P.M., 1979. Source of antioxidant activity of soybeans and soy products. J. Food Sci. 44, 1720–1722. https://doi.org/10.1111/j.1365-2621.1979.tb09125.x.

Qi, B., Yao, R., 2007. L-lactic acid production from *Lactobacillus casei* by solid state fermentation using rice straw. BioResources 2, 419–429. https://doi.org/10.15376/biores.2.3.419-429.

Rehal, J., Beniwal, V., Gill, B.S., 2019. Physico-chemical, engineering and functional properties of two soybean cultivars. Legum. Res. 42, 39–44. https://doi.org/10.18805/lr.v0iOF.9109.

Rodríguez de Olmos, A., Correa Deza, M.A., Garro, M.S., 2017. Selected lactobacilli and bifidobacteria development in solid state fermentation using soybean paste. Rev. Argent. Microbiol. 49, 62–69. https://doi.org/10.1016/j.ram.2016.08.007.

Santos da Silveira, J., Durand, N., Lacour, S., Belleville, M.P., Perez, A., Loiseau, G., Dornier, M., 2019. Solid-state fermentation as a sustainable method for coffee pulp treatment and production of an extract rich in chlorogenic acids. Food Bioprod. Process. 115, 175–184. https://doi.org/10.1016/j.fbp.2019.04.001.

Su, L., Cheng, Y., Hsiao, F.S., Han, J.-C., Yu, Y.-H., 2018. Optimization of mixed solid-state fermentation of soybean meal by *Lactobacillus* species and *Clostridium butyricum*. Polish J. Microbiol. 67, 297–305.

Sulieman, A.A., Zhu, K.-X., Peng, W., Hassan, H.A., Mahdi, A.A., Zhou, H.-M., 2019. Influence of fermented and unfermented *Agaricus bisporus* polysaccharide flours on the antioxidant and structural properties of composite gluten-free cookies. LWT - Food Sci. Technol. J. 101, 835–846. https://doi.org/10.1016/j.lwt.2018.11.007.

Wang, X., Qin, L., Zhou, J., Li, Y., Fan, X., 2018. A novel design to screen chlorogenic acid-producing microbial strains from the environment. Sci. Rep. 8, 1–10. https://doi.org/10.1038/s41598-018-32968-0.

Wondimkun, Z.T., Jebessa, A.G., Molloro, L.H., Haile, T., 2016. The determination of caffeine level of Wolaita Zone, Ethiopia coffee using UV-visible spectrophotometer. Am. J. Appl. Chem. 4, 59–63. https://doi.org/10.11648/j.ajac.20160402.14.

Yun, N., Kang, J.W., Lee, S.M., 2012. Protective effects of chlorogenic acid against ischemia/reperfusion injury in rat liver: molecular evidence of its antioxidant and anti-inflammatory properties. J. Nutr. Biochem. 23, 1249–1255. https://doi.org/10.1016/j.jnutbio.2011.06.018.

Zamindar, N., Bashash, M., Khorshidi, F., Serjouie, A., Shirvani, M.A., Abbasi, H., Sedaghatdoost, A., 2017. Antioxidant efficacy of soybean cake extracts in soy oil protection. J. Food Sci. Technol. 54, 2077–2084. https://doi.org/10.1007/s13197-017-2646-0.

Zhang, S.T., Shi, Y., Zhang, S.L., Shang, W., Gao, X.Q., Wang, H.K., 2014. Whole soybean as probiotic lactic acid bacteria carrier food in solid-state fermentation. Food Control 41, 1–6. https://doi.org/10.1016/j.foodcont.2013.12.026.

Zhou, G., Ma, J., Tang, Y., Wang, X., Zhang, J., Yao, X., Jiang, W., Duan, J.-A., 2018. Optimization of ultrasound-assisted extraction followed by macroporous resin purification for maximal recovery of functional components and removal of toxic components from *Ginkgo biloba* leaves. Biomed Res. Int. 2018, 1–15. https://doi.org/10.1155/2018/4598067.